

# Cost-Optimal ATCs in Zonal Markets

Tue Vissing Jensen, *Student Member, IEEE*, Jalal Kazempour, *Member, IEEE*,  
and Pierre Pinson, *Senior Member, IEEE*

**Abstract**—In contrast to existing frameworks for Available Transfer Capacity (ATC) determination, we propose to define ATCs in an integrated and data-driven manner, optimizing for expected operational costs of the whole system to derive *cost-optimal* ATCs. This requires viewing ATCs as an endogenous market construct, and leads naturally to the definition of a market entity whose responsibility is to optimize ATCs. The optimization problem which this entity solves is a stochastic bilevel problem, which we decompose to yield a computationally tractable formulation. We show that cost-optimal ATCs depend non-trivially on the underlying network structure, and the problem of finding a set of cost-optimal ATCs is in general non-convex. On a European-scale test system, cost-optimal ATCs achieve expected total costs midway between those for non-integrated ATCs and a fully stochastic nodal setup. This benefit comes from qualitatively different ATCs compared to typical definitions, with ATCs which exceed the physical cross-border capacity by a factor of 2 or more, and ATCs which are zero between well-connected areas. Our results indicate that the perceived efficiency gap between zonal and nodal markets may be exaggerated if non-optimal ATCs are used.

**Index Terms**—Zonal Electricity Markets, Market Coupling, Available Transfer Capacity, Bilevel programming

## NOMENCLATURE

### A. Sets

$z \in Z$	Set of zones
$n \in N$	Set of nodes
$N_{SI} \subseteq N$	Set of slack buses
$g \in G$	Set of generators
$G_z \subseteq G$	Set of generators in zone $z$
$G_n \subseteq G$	Set of generators at node $n$
$e \in E$	Set of links in zonal network
$z \rightarrow \subseteq E$	Set of links originating from zone $z$
$\rightarrow z \subseteq E$	Set of links ending at zone $z$
$l \in L$	Set of lines in transmission network
$n \rightarrow \subseteq L$	Set of lines originating from node $n$
$\rightarrow n \subseteq L$	Set of lines ending at node $n$
$\omega \in \Omega$	Set of scenarios for renewable production

### B. Variables

Variables indexed by  $\omega$  refer to real-time (RT) markets.

$p_g^{\text{DA}} (p_{g\omega}^{\text{RT}})$	Production of generator $g$ [MW]
$p_{g\omega}^{\uparrow}, p_{g\omega}^{\downarrow}$	Up/down regulation of generator $g$ [MW]
$w_z^{\text{DA}} (w_{n\omega}^{\text{RT}})$	Scheduled renewable production in zone $z$ / node $n$ [MW]
$f_e^{\text{DA}} (f_{l\omega}^{\text{RT}})$	Flow on link $e$ / line $l$ [MW]

T. Jensen, J. Kazempour and P. Pinson are with the Technical University of Denmark, 2800 Kgs. Lyngby DK (e-mail: {tvjens, seykaz, ppin}@elektro.dtu.dk)

This work is partly funded by ‘5s’ — Future Electricity Markets (12-132636/DSF).

$J_z^{\text{s,DA}} (J_{n\omega}^{\text{s,RT}})$	Load shed in zone $z$ / node $n$ [MW]
$ATC_e$	Flow limit for link $e$ [MW]
$\theta_{n\omega}$	Phase angle in node $n$ [rad]
$\text{Cost}^{\text{DA}}$	Total dispatch cost in the day-ahead market [\\$]
$\Delta \text{Cost}_{\omega}^{\text{RT}}$	Change in dispatch cost from real-time operation in scenario $\omega$ [\\$]
$\alpha_{\omega}$	Benders’ proxy variable [\\$]

### C. Parameters

$p_g^{\text{max}}$	Capacity of generator $g$ [MW]
$\pi_g$	Price offer of generator $g$ [\$/MWh]
$W_z^{\text{DA}}$	Day-ahead renewable offer in zone $z$ [MW]
$\pi^{\text{r}}$	Price offer of renewables [\$/MWh]
$W_{n\omega}^{\text{RT}}$	Realized renewable production at node $n$ [MW]
$L_z^{\text{DA}}$	Projected load in zone $z$ [MW]
$L_n^{\text{RT}}$	Realized load at node $n$ [MW]
$F_l^{\text{max}}$	Physical flow limit on line $l$ [MW]
$B_l$	Susceptance of line $l$ [p.u.]
$VOLL$	Value of lost load [\$/MWh]
$\phi_{\omega}$	Probability of scenario $\omega$
$\alpha^{\text{min}}$	Lower bound to Benders’ proxy variable [\\$]

## I. INTRODUCTION

AS renewable penetration increases, the cost of compensating for its uncertainty comes to dominate electricity market operation costs [1]. A major challenge in modern electricity market design is how to properly account for this uncertainty to optimally integrate renewable production [2]. This challenge is even greater in a European context, where prices cannot be directly differentiated by their geographical location, but must be the same across pre-defined market areas, i.e., *zones*, often an entire country [3]. Under this restriction on prices, any method for which the day-ahead price seen by a market participant can depend on its location inside the zone is untenable. Such methods include stochastic market designs in the vein of [4] and [5] with full network representation, which in this context are the ideal benchmark in terms of expected system cost. The primary degree of freedom left to influence the dispatch is to control the maximal commercial exchange between zones, known as the available transfer capacity, or ATC.<sup>1</sup>

While these ATCs are historically set based on measures of security irrespective of their market use [7], [8], they influence market clearing. This interaction has not been extensively explored. One question which has yet to be fully examined is to which extent the chosen ATCs impact market outcomes,

<sup>1</sup>Depending on context, the same concept has been referred to as Net Transfer Capacity (NTC) or Total Transfer Capacity (TTC). See [6] for a disambiguation.

and whether market efficiency can be improved by changing our view of ATCs. To quantify the efficiency gap between the best possible zonal market and the ideal benchmark of a stochastic nodal market, the best possible ATCs for the zonal market must be uncovered, while taking renewable uncertainty into account.

Previous works on the connection between the definition of ATCs and market outcomes have focused on ATCs as a technical construct derived from the underlying network. In [9], ATCs are defined statically depending only on the network topology, as the maximal two-zone transfer which is robust to the intra-zonal injection pattern. In [10], ATCs are defined according to the expected operating point as the maximal deviation in transfer such that the system is robust. Both methods define ATCs exogenously without reference to their use in market clearing. The work of [11] uses grid search to find the ATC which leads to lowest overall cost for a two-node topology. This method does not scale to large grids, and may not achieve global optimality.

To address these issues, we examine a method of ATC determination for a given topology of zones based on a stochastic setup which (i) uses explicit information on the uncertainty of variable renewable production (VRES, here wind and solar), (ii) respects the zonal pricing system currently in use in European markets, (iii) minimizes the expected total cost of operating the system under renewable uncertainty while respecting transmission limits, and (iv) is computationally tractable for large-scale problems. These features are achieved by setting the ATCs between zones to indirectly control the dispatch of generators towards a dispatch that is better suited to deal with the forecast renewable uncertainty. The resulting ATCs are a purely financial construct, which, though derived from the physical underlying system, do not have to correspond to the thermal limits of the underlying transmission lines, and may in some cases exceed them. The proposed method can be brought closer to current practice by including, e.g., minimum ATCs at the cost of sub-optimality.

Compared to [9], our method determines ATCs which optimally account for scenarios of net load situation, and defines ATCs based on their use in day-ahead markets. Next to [10], we treat ATCs as endogenous to our day-ahead market model, and evaluate them under renewable uncertainty. Our results complement the conclusions of [10] by showing that the perceived performance of zonal market depend on the chosen ATCs. In contrast to [11], our method extends to large-scale systems, and is guaranteed to find a set of ATCs which attain the minimum global expected cost.

The rest of this paper is organized as follows. Section II expands on current ATC practice and introduces the assumptions used for our method. Section III gives the method formulation and its decomposed form. Section IV examines two case studies to reveal features of the problem and its outcomes. Finally, Section V concludes on the results obtained.

## II. PRELIMINARIES AND ASSUMPTIONS

### A. ATC Definition: Current Practice

The appeal of using generation resources more efficiently across borders and integrating more renewables, drives the

coupling of the European electricity system [12]. The physical system comprises several thousand buses  $n \in N$  and transmission lines  $l \in L$  across the continent. By contrast, in current European day-ahead markets, the transmission grid is simplified to interconnections  $e \in E$  between tens of market zones  $z \in Z$ . This simplified zonal view of the transmission system in the day-ahead market stage challenges system operation, as it does not represent the physical nodal transmission system [9], [13]. Reconciling these zonal and nodal descriptions constitutes unique challenges in market design [9]–[11]. Of particular importance is examining how market zones interact, as efficient trade between market zones lowers system operation cost [12].

When clearing day-ahead markets, market operators of each zone can clear bids across links  $e$ , limited by the corresponding  $ATC_e$ . Efficient market operation requires properly defining the ATCs. Their definition involves a trade-off between efficient trading of energy and system reliability: If ATCs are too restrictive, fewer trades may be cleared, leading to a loss of social welfare (increased system cost). On the other hand, if ATCs are too lax, too much energy may be scheduled to be transmitted across some lines, which may force use of expensive balancing resources or endanger system reliability.

Historically, Transmission System Operators (TSOs) have defined ATCs from a security standpoint; Given the expected system operating points, find the maximal transfer of energy across the link  $e$ ,  $f_e$ , that will allow the system to operate securely [10]. Several reliability indices have been proposed to quantify the stability and security of the system, such as loss of load probability and energy not supplied, analyzed under contingencies [7], [8]. Though European markets have in recent years moved from ATC-based day-ahead market coupling to flow-based market coupling [6], the security-based view of market coupling is unchanged. Thus, in current practice ATCs are fundamentally taken to be a technical construct; they represent the physical capabilities of the underlying grid without reference to their use in market clearing and the resulting financial impacts.

However, ATCs are fundamentally a *financial* concept: they inform market participants how much trade between zones is beneficial to the system as a whole. From this perspective, ATCs are not tightly coupled to the physical grid; so long as the day-ahead trades carried out using ATCs result in a feasible and efficient dispatch in real-time, TSOs should not care what their specific values are. This view suggests that by decoupling ATC definition from the physical grid to some extent, it may be possible for the European system to operate at lower overall cost by optimizing ATCs, a suggestion supported by our findings in this paper. We refer to the optimized ATCs as cost-optimal, opposed to the commonly used non-integrated ATCs. The following subsection builds the machinery needed to define cost-optimal ATCs.

### B. ATCs as Degrees of Freedom

A given set  $\{ATC_e\}_{e \in E}$  of ATCs determine final costs through day-ahead market trading decisions and redispatch needs, as shown in Fig. 1. In order to lower the final expected cost (system cost in day-ahead, i.e.,  $\text{Cost}^{\text{DA}}$ , plus the mean cost

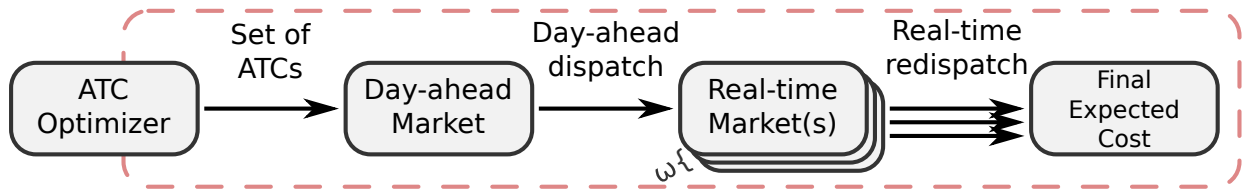


Fig. 1. Functioning of a zonal market structure. Each arrow indicates the outcome of a step, which is input to the following step. The real-time market(s) clear depending on the realized scenario  $\omega$ . The dashed box indicates the problem of the ATC optimizer.

of balancing actions, i.e.,  $\sum_{\omega} \phi_{\omega} \Delta \text{Cost}_{\omega}^{\text{RT}}$ , one can consider this diagram as a feedback loop; for any proposed  $\{ATC_e\}_{e \in E}$ , the final expected cost changes. If the purpose of the market is to minimize final expected cost, this feedback loop should be used to determine ATCs.

This endogenous approach defines the *ATC optimizer's problem*: Given a belief about day-ahead offers, balancing offers and possible net load scenarios, find  $\{ATC_e\}_{e \in E}$  which leads to the lowest expected cost of operation. The ATC optimizer is a market entity who acts as the leader in a Stackelberg game, anticipating the day-ahead market and real-time market(s) acting as sequential followers. Stackelberg games are naturally formulated as bilevel optimization problems [14], with the upper level representing the ATC optimizer's (leader's) problem of defining a set of ATCs, and the lower-level problems (followers) representing the day-ahead market clearing and the real-time balancing action, respectively.

Formally, the ATC optimizer's problem is written as

$$\min_{ATC_e} \text{Cost}^{\text{DA}} + \sum_{\omega} \phi_{\omega} \Delta \text{Cost}_{\omega}^{\text{RT}} \quad (1a)$$

$$\text{s.t. } ATC_e \geq 0 \quad \forall e \in E \quad (1b)$$

$$\text{Cost}^{\text{DA}} \in (2) \quad (1c)$$

$$\Delta \text{Cost}_{\omega}^{\text{RT}} \in (3)_{\omega} \quad \forall \omega \in \Omega \quad (1d)$$

where minimizing final expected cost (1a) determines the optimal non-negative ATCs (1b). Anticipated system costs in day-ahead (1c) and balancing costs in real-time per scenario (1d) are given by lower-level problems. The ATC optimizer must solve (1) for every time period under consideration.

We do not propose that European market operators rush out to employ ATC optimizers, but rather view the definition of such a market position as an interesting theoretical construct: The set of ATCs which the ATC optimizer finds yield a lower bound on the cost of operating the zonal market, i.e. it is a fundamental limitation on zonal market clearing as practiced in Europe today. The approach considered here can then be used to assess the efficiency of a zonal market: The closer a zonal market's cost is to the ATC optimizer's optimum, the better the market functions.

### C. Modeling Assumptions and Problem Structure

In order to formulate this problem in a tractable manner, assumptions on the associated market clearings are necessary.

The day-ahead market is assumed to clear in a fully coordinated fashion, where each zone is assumed to be an energy exchange which allows partial acceptance of offers.

Renewables are assumed to offer their mean into the day-ahead market at zero price ( $\pi_r = \$0/\text{MWh}$ ) and are the only source of uncertainty in the system. The ATC optimizer uses a forecast of real-time VRES production in the day-ahead stage to assess the costs incurred for redispatching.

We use the term 'real-time market' for any mechanism which modifies the day-ahead dispatch after it is given. The net effect of these mechanisms is to re-dispatch the system to an operation point that is feasible with respect to the full nodal transmission description and actual production of renewable sources. We employ the usual DC flow description for the nodal transmission model, and assume generators are re-dispatched in the cheapest possible manner, that is, the real-time market is fully coordinated between zones.

Each generator  $g$  is assumed to offer into the real-time market at a price that differs from its marginal cost (day-ahead offer) by  $\pi_g^+$  for up-regulation and  $\pi_g^-$  for down-regulation, such that it is more expensive to re-dispatch a generator closer to real-time. We do not consider inter-temporal constraints such as ramp limits and storage, or non-convexities in costs associated with unit commitment decisions, assuming that these are represented by the generators through their offer prices. These assumptions make the day-ahead and real-time market clearing problem convex, which is necessary for our formulation. Even though this structure for real-time markets is simplified compared to, e.g., [10] it suffices to examine the impact of endogenous ATC definition.

We neglect strategic behavior of market participants in general, and in particular with respect to the updated ATCs, and assume that the ATC optimizer's offer estimates for the day-ahead market are the offers that end up being given in the day-ahead market. Further, we do not model forward and bilateral markets, whose trades would in practice not be known to the ATC optimizer in advance. As with any approach which assumes perfect information, our method depends upon the belief of market parameters, and produces optimal ATCs accordingly.

The next section formulates the ATC-optimizer's problem as an optimization problem, and builds a computationally tractable version by decomposition.

## III. PROPOSED MODEL

### A. Problem Formulation

As shown in Fig. 1, the ATC optimizer seeks a set of ATCs which minimize the expected cost of operation, when all participants trade in the day-ahead market with those ATCs, and a corrective action happens in real-time. The ATC

optimizer must solve its problem under its belief about the day-ahead (DA) and real-time (RT) correction per scenario.

Building on the sketch in (1), we need to explicitly define the day-ahead and real-time market clearing problems. To this end, given a set of ATCs, the zonal network is used to clear the day-ahead market as

$$\begin{aligned}
 \min_{\Xi^{\text{DA}}} \quad & \text{Cost}^{\text{DA}} = \sum_g \pi_g p_g^{\text{DA}} \\
 & + \sum_z \text{VOLL}_z l_z^{\text{s,DA}} + \pi^r \sum_z w_z^{\text{DA}} \quad (2a) \\
 \text{s.t.} \quad & \sum_{g \in G_z} p_g^{\text{DA}} + w_z^{\text{DA}} + l_z^{\text{s,DA}} = L_z^{\text{DA}} + \\
 & + \sum_{e \in z \rightarrow} f_e^{\text{DA}} - \sum_{e \in \rightarrow z} f_e^{\text{DA}} \quad \forall z \in Z \quad (2b) \\
 & 0 \leq p_g^{\text{DA}} \leq p_g^{\text{max}} \quad \forall g \in G \quad (2c) \\
 & 0 \leq w_z^{\text{DA}} \leq W_z^{\text{DA}} \quad \forall z \in Z \quad (2d) \\
 & 0 \leq l_z^{\text{s,DA}} \leq L_z^{\text{DA}} \quad \forall z \in Z \quad (2e) \\
 & -\text{ATC}_e \leq f_e^{\text{DA}} \leq \text{ATC}_e \quad \forall e \in E \quad (2f)
 \end{aligned}$$

which yields a day-ahead dispatch  $p_g^{\text{DA}}$ . The variable set  $\Xi^{\text{DA}} = \{p_g^{\text{DA}}, w_z^{\text{DA}}, l_z^{\text{s,DA}}, f_e^{\text{DA}}\}$  includes the day-ahead dispatch per generator, scheduled renewable energy, load shed and flow on each zonal link, respectively.

The objective function (2a) minimizes the DA cost, including generation costs of conventional and renewable producers, plus load shedding costs. As renewable energy is treated uniformly across the zone, we simply operate with one renewable production variable per zone. The DA power balance per zone is given by (2b), with subsequent constraints giving bounds on each DA variable. Note that in (2f),  $\text{ATC}_e$  are the ATCs determined in (1). Though they are variables in (1), they are treated as parameters in (2).

Similarly, the RT redispatch model for each scenario  $\omega$  is written as

$$\begin{aligned}
 \min_{\Xi^{\text{RT}}} \quad & \Delta \text{Cost}_{\omega}^{\text{RT}} \quad (3a) \\
 & = \sum_g (\pi_g (p_{g\omega}^{\text{RT}} - p_g^{\text{DA}}) + \pi_g^+ p_{g\omega}^+ + \pi_g^- p_{g\omega}^-) \\
 & + \sum_n \text{VOLL}_n l_{n\omega}^{\text{s,RT}} + \pi^r \sum_n w_{n\omega}^{\text{RT}} \\
 & - \left[ \sum_z \text{VOLL}_z l_z^{\text{s,DA}} + \pi^r \sum_z w_z^{\text{DA}} \right] \\
 \text{s.t.} \quad & \sum_{g \in G_n} p_{g\omega}^{\text{RT}} + w_{n\omega}^{\text{RT}} + l_{n\omega}^{\text{s,RT}} = L_n^{\text{RT}} + \\
 & + \sum_{l \in n \rightarrow} f_{l\omega}^{\text{RT}} - \sum_{l \in \rightarrow n} f_{l\omega}^{\text{RT}} \quad \forall n \in N \quad (3b)
 \end{aligned}$$

$$p_{g\omega}^{\text{RT}} = p_g^{\text{DA}} + p_{g\omega}^+ - p_{g\omega}^- \quad \forall g \in G \quad (3c)$$

$$f_{l\omega}^{\text{RT}} = B_l (\theta_{n\omega} - \theta_{m\omega}) \quad \forall (n, m) = l \in L \quad (3d)$$

$$0 \leq p_{g\omega}^{\text{RT}} \leq p_g^{\text{max}} \quad \forall g \in G \quad (3e)$$

$$0 \leq w_{n\omega}^{\text{RT}} \leq W_{n\omega}^{\text{RT}} \quad \forall n \in N \quad (3f)$$

$$0 \leq l_{n\omega}^{\text{s,RT}} \leq L_n^{\text{RT}} \quad \forall n \in N \quad (3g)$$

$$-F_l^{\text{max}} \leq f_{l\omega}^{\text{RT}} \leq F_l^{\text{max}} \quad \forall l \in L \quad (3h)$$

$$\theta_{n\omega} = 0 \quad \forall n \in N_{\text{Sl}} \quad (3i)$$

where  $\Xi^{\text{RT}} = \{p_{g\omega}^{\text{RT}}, p_{g\omega}^+, p_{g\omega}^-, w_{n\omega}^{\text{RT}}, l_{n\omega}^{\text{s,RT}}, f_{l\omega}^{\text{RT}}, \theta_{n\omega}\}$  contains the real-time generator dispatch, the up- and down-regulation per generator, the delivered renewable production, load shed, flow per transmission line and voltage phase angle.

Objective function (3a) minimizes the RT rebalancing cost, including the regulation costs of generators and load shedding costs. The power balance per node is given by (3b). The coupling of the DA and RT schedules through balancing actions is given by (3c), while transmission flows are given in (3d). Equations (3e)–(3i) define bounds on the RT decision variables and zeros the phase angle of each slack bus. In particular, (3h) restricts the flow on a line to its actual capacity. Note that the upper bound of (3f), i.e.,  $W_{n\omega}^{\text{RT}}$ , is the uncertain parameter which differs from scenario to scenario. The day-ahead dispatch variables  $p_g^{\text{DA}}, l_z^{\text{s,DA}}$  and  $w_z^{\text{DA}}$  are received from (2), and treated as parameters in the RT problem.

## B. Problem Decomposition

Both lower-level problems (2) and (3) are linear and thus convex, so their Karush-Kuhn-Tucker (KKT) conditions are optimality conditions. However, a naive implementation of (1) which replaces (2) and (3) by their KKT conditions would result in a computationally intractable problem. In order to allow our method to solve problems of a realistic size, it is necessary to decompose (1) into smaller problems — in this particular problem, we decompose problem (1) by scenario.

For a fixed DA dispatch, the constraints in (1) are independent per scenario. This allows rewriting the problem using Bender's decomposition, where the subproblems are the RT redispatch problems. Taking the complicating (fixing) variables to be  $p_g^{\text{DA}}$ , we write Benders' subproblem at iteration  $m$  for scenario  $\omega$  as

$$\min_{\Xi^{\text{RT}}} \quad \Delta \text{Cost}_{\omega}^{\text{RT}} \quad (4a)$$

$$\text{s.t.} \quad p_g^{\text{DA}} = p_g^{\text{DA};(m)} : \gamma_{g,\omega}^{(m)} \quad \forall g \in G \quad (4b)$$

$$\Xi^{\text{RT}} \in (3)_{\omega} \quad (4c)$$

where the dual variable  $\gamma_{g,\omega}^{(m)}$  is the sensitivity to the DA dispatch of generator  $g$ , used for generating Benders' cuts. The subscript  $\omega$  in (4c) indicates the corresponding problem for the given scenario.

As the objective function in (4) is the same as in (3), the bilevel structure of subproblem (4) collapses to

$$\min_{\Xi^{\text{RT}}} \quad \Delta \text{Cost}_{\omega}^{\text{RT}} \quad (5a)$$

$$\text{s.t.} \quad (3b)_{\omega} - (3i)_{\omega}$$

$$p_g^{\text{DA}} = p_g^{\text{DA};(m)} : \gamma_{g,\omega}^{(m)} \quad \forall g \in G \quad (5b)$$

The resulting subproblem is convex as a function of the DA dispatch, which guarantees that the decomposed problems converge to the optimal solution of the non-decomposed problem (1) [15].

The Benders' master problem in iteration  $m$  is

$$\min_{\substack{\text{Cost}^{\text{DA}} + \sum_{\omega} \phi_{\omega} \alpha_{\omega} \\ \alpha_{\omega} \geq \alpha^{\min} \quad \forall \omega \in \Omega}} \quad (6a)$$

$$\text{s.t.} \quad \alpha_{\omega} \geq \alpha^{\min} \quad \forall \omega \in \Omega \quad (6b)$$

$$\alpha_{\omega} \geq \Delta \text{Cost}_{\omega}^{\text{RT};(i)} + \sum_g \gamma_{g,\omega}^{(i)} (p_g^{\text{DA}} - p_g^{\text{DA};(i)}) \quad (6c)$$

$$\forall i \in \{1, \dots, m-1\}, \omega \in \Omega \quad (6c)$$

$$\text{Cost}^{\text{DA}} \in (2) \quad (6d)$$

$$\text{ATC}_e \geq 0 \quad \forall e \in E \quad (6e)$$

where  $\cdot^{(i)}$  indicates the variable's fixed value at iteration  $i$ . The proxy variable  $\alpha_{\omega}$  represents the RT redispatch cost under scenario  $\omega$ . The optimality cuts in (6c) are from Benders' multicut method [16], which was found to yield faster convergence in our applications. As the subproblems (5) are always feasible for any fixed DA dispatch, no feasibility cuts are necessary in (6). The Benders' iterations converge in iteration  $m$  if  $\sum_{\omega} \phi_{\omega} \alpha_{\omega}^{(m)} = \sum_{\omega} \phi_{\omega} \Delta \text{Cost}_{\omega}^{\text{RT};(m)}$  to within tolerance.

Note that Benders' master problem (6) still has a bilevel structure. It is transformed by replacing the lower-level optimization problem (6d) by its KKT conditions, and reformulating these using the standard Big-M method [17], yielding a mixed-integer linear programming problem which we omit here for brevity.

Two modifications are made to (5) and (6) to reduce complexity and handle degeneracy. First, to reduce the number of variables exchanged between master and subproblems, we redefine for each scenario  $\omega$

$$\begin{aligned} \Delta \text{Cost}_{\omega}^{\text{RT}} = & \sum_g (\pi_g (p_{g\omega}^{\text{RT}} - p_g^{\text{DA}}) + \pi_g^+ p_{g\omega}^+ + \pi_g^- p_{g\omega}^-) \\ & + \sum_n \text{VOLL}_n l_n^{\text{s,RT}} + \pi^r \sum_n w_{n\omega}^{\text{RT}}, \end{aligned} \quad (7)$$

which is equivalent to (3a) with the term in square brackets removed. We move this term to Benders' cuts, (6c), which now writes as

$$\begin{aligned} \alpha_{\omega} \geq & \Delta \text{Cost}_{\omega}^{\text{RT};(i)} + \left[ \sum_z \text{VOLL}_z l_z^{\text{s,DA};(i)} + \pi^r \sum_z w_z^{\text{DA};(i)} \right] + \\ & + \sum_g \gamma_{g,\omega}^{(i)} (p_g^{\text{DA}} - p_g^{\text{DA};(i)}) \quad \forall i \in \{1, \dots, m-1\}, \omega \in \Omega \end{aligned} \quad (8)$$

As a result, only the DA schedule of conventional generators ( $p_g^{\text{DA}}$ ) needs to be shared between master and subproblems.

Second, in solving the above problem, it may happen that some ATC constraints are not binding. This leads to an unbounded ray, where the cost does not change when the ATC goes to infinity. To avoid this, we add the penalty term  $\epsilon \sum_e \text{ATC}_e$  to (6a), where  $\epsilon$  is a small value, e.g.,  $10^{-6}$ . This term ensures that among possible ATCs which lead to a degenerate cost, the smallest ATC is chosen. We proceed to apply this final formulation to a series of test cases.

#### IV. CASE STUDIES

To show the results of optimizing ATCs, we employ two test cases. By first calculating the optimal set of ATCs for a small test system, we show that the method is sensitive to

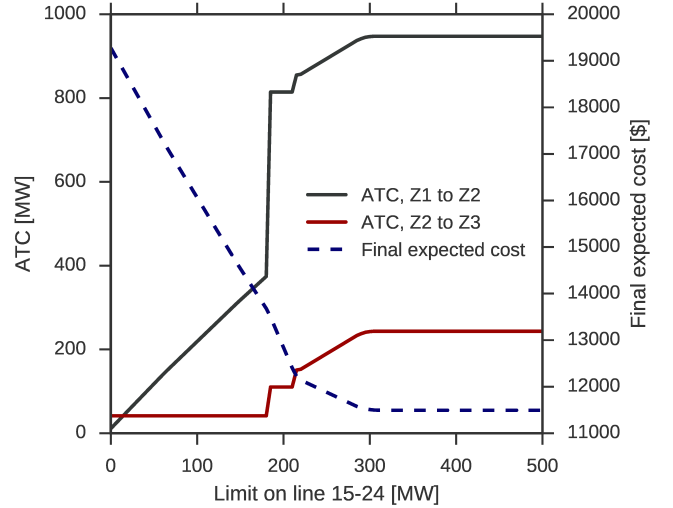


Fig. 2. The 24-bus IEEE reliability test system: Cost-optimal ATCs found by the proposed formulation (left axis) and final expected cost (right axis) as a function of the capacity on the line 15–24.

TABLE I  
ZONES FOR IEEE RELIABILITY TEST SYSTEM

	Zone 1	Zone 2	Zone 3
Nodes in zone	1, 2, 4–6	3, 7–14	15–24

having access to the precise information on the network. The second test system shows how our method scales to large-scale systems, and examines the impact of employing optimal ATCs on the expected total cost of operation. This second test system further demonstrates a lower bound on the efficiency of European zonal markets.

The optimization problems (5) and (6) were implemented in Python using the Gurobi solver package. This implementation solves the large-scale test case to a 1% Benders gap in 1–4 hours. All codes used are available at [18].

##### A. Test Case: IEEE 24-bus Reliability Test System

To verify the implementation and show some interesting features of the method, we use a modified version of the IEEE 24-bus reliability test system [19]. This system is divided into the three zones listed in Table I, and connected via two interconnections (links); one from zone 1 to zone 2, and one from zone 2 to zone 3. The low dimensionality of this system allows directly plotting final expected cost as a function of the ATCs on each link. For this example, we examine the cost-optimal ATCs for the first hour.

The modifications to the base system [19] are as follows: 50 MW of wind capacity is placed at each of nodes 3, 5, 7, 16, 21 and 23. Each wind generators' output per scenario is drawn independently from a Beta distribution with shape parameters  $\alpha = 2$  and  $\beta = 4$ . In total, 100 scenarios for wind generation are used to schedule the system. We assume redispatch premiums are  $\pi_g^+ = \$7.90/\text{MWh}$  and  $\pi_g^- = \$8.59/\text{MWh}$  independent of the generator. By varying the capacity limit on the line connecting nodes 15 and 24, both of which are inside zone 3,

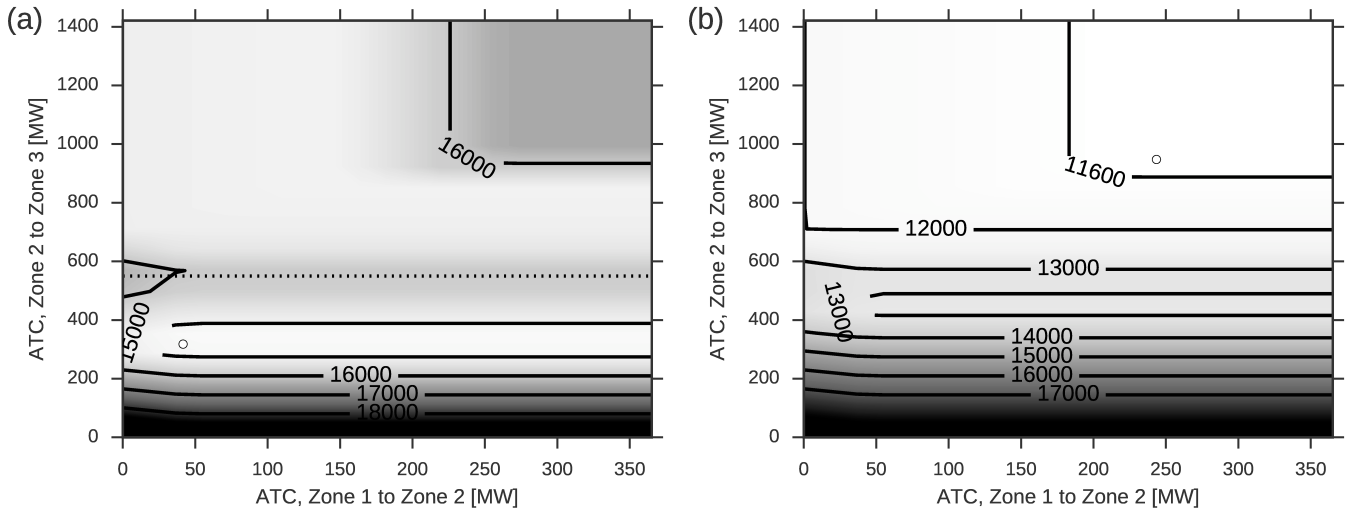


Fig. 3. The 24-bus IEEE reliability test system: Final expected cost [\$] as function of ATCs with the capacity on line 15–24 set to (a) 150 MW, (b) 500 MW. The circle indicates the cost-optimal ATCs found by the proposed formulation. The dotted line in (a) indicates a region of high cost separating two regions of lower cost.

we show the sensitivity of our method to network conditions. Fig. 2 shows the cost-optimal ATCs as a function of the thermal limit on line 15–24, together with the resulting final expected cost. The cost-optimal ATCs change drastically for capacity limits around 200MW, indicating that they depend non-trivially on actual network characteristics.

This is further indicated by Fig. 3, which shows final expected cost as a function of ATCs for two different capacities on the line connecting nodes 15 and 24. For a line capacity below 200MW, the optimal ATCs are in the lower left corner of Fig. 3 (a). In contrast, for a line capacity well above 200MW, the optimal set of ATCs are in the upper right corner of Fig. 3 (b). Between these two points there is a barrier of higher cost, indicated by the dotted line in Fig. 3 (a) at approximately 500MW on the vertical axis. As the line capacity increases from below 200MW to above, the optimal set of ATCs must cross this barrier, leading to the sudden change observed in Fig. 2. The existence of this barrier shows that final expected cost is in general a non-convex function of  $ATC_e$ .

This non-convexity of costs and cost-optimal ATCs indicates that our method of ATC determination is highly sensitive to the input data used to generate ATCs. Such sensitivity poses problems for any potential market design based on deriving cost-optimal ATCs, as small errors in the market information may lead to disproportionate errors in operational costs. This may be partially addressed by extending the method to optimize against scenarios of market conditions, e.g., offer price of conventional generators, in addition to wind scenarios.

### B. Test Case: European-Scale System Model

To examine the limitations of zonal pricing, we examine our model applied to the RE-Europe test system [20]. This test system contains 1500 nodes, 2000 lines and 969 generators, and comes with wind and solar point forecasts and signals at hourly resolution as well as hourly load signals. We use the

‘uniform’ capacity layout for wind and solar power, with a base scenario of 50% gross VRES penetration, of which 80% of yearly energy production comes from wind and 20% from solar. We generate scenarios from the supplied point forecasts from ECMWF data, with the real-time signal derived from the COSMO dataset, for details, see [20]. These scenarios have the correct empirical spatial dependence structure, while being uncoupled in time, which is of no importance in our formulation, see [18] for more details on scenario generation.

Each country in the test system is assumed to comprise a single market zone, and two zones are connected if they have a transmission line connecting them in the underlying grid. The resulting zonal configuration comprises 25 zones with 46 interconnections between them. These assumptions neglect the division of Italy and Denmark into separate bidding zones, anticipate the splitting of Austria and Germany into two separate zones as recommended in [21], and assumes all countries have national electricity markets, even though some do not.

Due to the size of the test system, we divide the problem by hours and solve for a cost-optimal ATC for each hour separately. This is in line with current practice in, e.g., Nordpool, where ATCs are updated hour by hour [22]. We arbitrarily choose to run simulations for each hour of the 15th of June 2014. As before, we assume redispatch premiums are  $\pi_g^+ = \$7.90/\text{MWh}$  and  $\pi_g^- = \$8.59/\text{MWh}$  independent of the generator. These values are the median-of-median differences between day-ahead and regulating prices in Nordpool for 2014 [22]. Our results are insensitive to an overall shift of these premiums, up to their trivial effect on redispatch costs. The specifics of our results may change if the premiums differ per generator, but we consider a full treatment of this effect outside the scope of this paper.

We compare our cost-optimized ATCs against (i) a stochastic nodal dispatch in which the nodal network is used in both DA and RT stages considering the full set of scenarios, (ii)

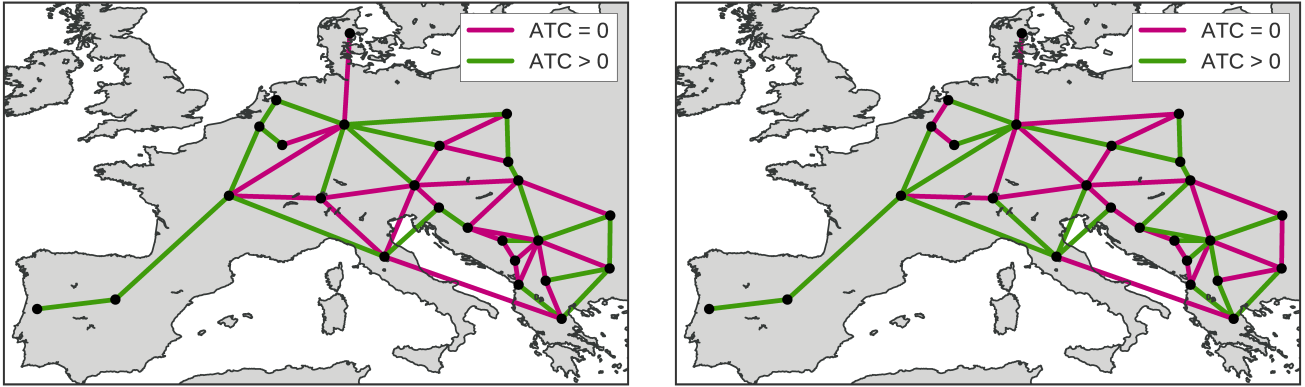


Fig. 5. European-scale system model: Qualitative map of cost-optimal ATCs found for (left) hour 17 and (right) hour 18.

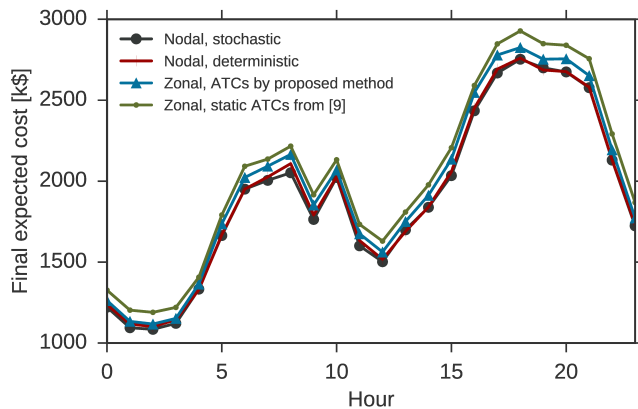


Fig. 4. European-scale system model: Final expected costs per hour.

TABLE II  
EUROPEAN-SCALE SYSTEM MODEL: MEAN HOURLY COST BY METHOD

	DA Cost [k\$]	Final expected cost [k\$]	% increase in final cost
Nodal, Stochastic (baseline)	3914	1901	—
Nodal, Deterministic	1558	1914	0.7
Zonal, Cost-optimal ATCs	1655	1970	3.6
Zonal, static ATCs from [9]	1928	2039	7.3

a deterministic nodal dispatch in which the uncertainty is ignored — the expected renewable production is considered as the single scenario, and (iii) a deterministic zonal dispatch using static ATCs derived as in [9]. Considering 10 scenarios, our proposed method generated cost-optimal ATCs, and the stochastic nodal model found an optimal DA schedule. The resulting DA schedule and ATCs were then evaluated using 100 scenarios, in which the previous 10 scenarios are included. Renewables are assumed to offer their mean production under the applicable scenarios into the DA market.

The resulting final expected costs are shown in Fig. 4, which shows that our method achieves an operational costs between the static ATCs and both nodal formulations for all hours considered. The mean of final expected cost over the horizon is given in Table II. The cost difference between the

TABLE III  
EUROPEAN-SCALE SYSTEM MODEL: EXAMPLE ATCs IN MW OBTAINED BY THE PROPOSED MODEL, THE METHOD OF [9] AND THE TOTAL CROSS-BORDER CAPACITY OF THE UNDERLYING GRID.

Link	Cost-optimal ATC hour 17	Cost-optimal ATC hour 18	Static ATC from [9]	Cross-border capacity
GER-FRA	0	10139	659	5130
ITA-FRA	13510	295	409	4880
ITA-SVN	2484	422	414	1949

stochastic and deterministic nodal models (0.7%) relates to the gain in efficiency from considering uncertainty directly. As the gap in final expected cost between the proposed formulation and the static ATCs is greater at 3.5%, our method achieves gains greater than would be expected from just considering VRES uncertainty. The use of static ATCs overestimates the efficiency gap between zonal and nodal markets by a factor of roughly 2.

However, this gain in efficiency comes with fundamentally different ATCs from today. Fig. 5 qualitatively shows the obtained cost-optimal ATCs for hours 17 and 18. Certain links receive an ATC of zero, preventing trades between the corresponding zones, with the closed-off links changing over time. This binary behavior extends to all hours considered, indicating that it is an inevitable part of defining cost-optimal ATCs. To examine the values in detail, a selection of optimal ATCs are tabulated in Table III. The GER-FRA link is closed for hour 17, but allows trades up to nearly twice the underlying grid strength in hour 18. In comparison, the ITA-FRA link displays the opposite trend; while initially open to trade for 2.5 times the underlying grid capacity, it reduces in hour 18 to less than the static ATC assignment. The cost-optimal ATC sizes do not always exhibit these extremes as shown by the ITA-SVN link, which fluctuates between 1.2 times the underlying grid strength and the static ATC assignment. The binary behavior shown in Fig. 5 and the fluctuations in Table III are due to the ATCs being used as indirect control of the dispatch. By constricting ATCs on certain links, zonal prices bring the DA dispatch closer to the ideal of the stochastic nodal model.

## V. CONCLUSIONS

We propose a method for defining cost-optimal ATCs, whereby an ATC optimizer finds the set of ATCs which lead to the lowest final expected cost under scenarios of renewable production. Analysis of a small test case demonstrated that the problem of finding cost-optimal ATCs for a given network and a given set of scenarios is in general a non-convex problem, which may be highly sensitive to available capacities on the underlying network. This sensitivity cautions against naively using cost-optimal ATCs in market designs.

Examining a European scale test system found that our method reduced final expected cost on a daily horizon by 3.5% compared to a static ATC assignment. Compared to the result of a full nodal model with and without stochastic DA market clearing, final expected costs increase by 3.6% and 2.9% respectively. The cost-optimal ATCs found are radically different than those corresponding to current practice, with many connections being closed for trades in one hour, but open for trades in the next. Due to the nature of the test case, the limited time span examined, and the simplified method used to generate the scenarios, one should be careful not to take these numbers as generally representative of the performance gains possible using our method. The numbers do, however, show that the method used to define ATCs may impact the perceived efficiency of zonal market clearing, inviting caution when non-integrated ATCs are used to make strong claims about the efficiency of zonal markets.

To further examine the limitations of zonal markets, the method employed here may be extended to make the definition of the market areas endogenously. Allowing dynamic zoning can only serve to further decrease costs, as using a single fixed topology provides an upper bound to this extension. Further, from a practical standpoint, though cost-optimal ATCs optimize for the highest overall social welfare, some zones may incur a welfare loss. To counteract this, cost-optimal ATCs may be extended to ensure no zone incurs a loss of social welfare from the defined ATCs, either directly or through an uplift system. Further extensions of interest are extending the ATC optimizer's problem to allocate reserves, and to reconcile the conceptual gap between non-integrated and cost-optimal ATCs.

## ACKNOWLEDGMENT

The authors would like to thank Stefanos Delikaraoglou (Technical University of Denmark) and Brent Eldridge (Johns Hopkins University) for enlightening discussions, and Christos Ordoudis (Technical University of Denmark) for his comments on the final manuscript.

## REFERENCES

- [1] J. M. Morales, M. Zugno, S. Pineda, and P. Pinson, "Electricity market clearing with improved scheduling of stochastic production," *Eur. J. Oper. Res.*, vol. 235, no. 3, pp. 765–774, Jun. 2014.
- [2] P. Pinson, "Wind energy: Forecasting challenges for its operational management," *Stat. Sci.*, vol. 28, no. 4, pp. 564–585, 2013.
- [3] ACER, "The influence of existing bidding zones on electricity markets," vol. 386, no. 34114458, pp. 1–16, 2013.
- [4] F. Bouffard, F. D. Galiana, and A. J. Conejo, "Market-clearing with stochastic security – Part I: Formulation," *IEEE Trans. Power Syst.*, vol. 20, no. 4, pp. 1818–1826, 2005.
- [5] J. M. Morales, A. J. Conejo, and K. Liu, "Pricing electricity in pools with wind producers," *IEEE Trans. Power Syst.*, vol. 27, no. 3, pp. 1366–1376, 2012.
- [6] K. Van den Bergh, J. Boury, and E. Delarue, "The flow-based market coupling in central western Europe: Concepts and definitions," *Electr. J.*, vol. 29, no. 1, pp. 24–29, Jan. 2016.
- [7] Y. Ou and C. Singh, "Assessment of available transfer capability and margins," *IEEE Trans. Power Syst.*, vol. 17, no. 2, pp. 463–468, May 2002.
- [8] L. Min and A. Abur, "Total transfer capability computation for multi-area power systems," *IEEE Trans. Power Syst.*, vol. 21, no. 3, pp. 1141–1147, 2006.
- [9] G. Oggioni, F. Murphy, and Y. Smeers, "Evaluating the impacts of priority dispatch in the European electricity market," *Energy Econ.*, vol. 42, pp. 183–200, Mar. 2014.
- [10] I. Aravena and A. Papavasiliou, "Renewable energy integration in zonal markets," *IEEE Trans. Power Syst.*, to be published.
- [11] J. Egerer, J. Weibezahn, and H. Hermann, "Two price zones for the German electricity market – Market implications and distributional effects," *Energy Econ.*, to be published, 2016.
- [12] The European Commission, *EU Energy Markets in 2014, 2014*. [Online]. Available: [http://ec.europa.eu/energy/sites/ener/files/documents/2014\\_energy\\_market\\_en.pdf](http://ec.europa.eu/energy/sites/ener/files/documents/2014_energy_market_en.pdf)
- [13] J. Dijk and B. Willems, "The effect of counter-trading on competition in electricity markets," *Energy Policy*, vol. 39, no. 3, pp. 1764–1773, 2011.
- [14] S. A. Gabriel, A. J. Conejo, J. D. Fuller, B. F. Hobbs, and C. Ruiz, *Complementarity Modeling in Energy Markets*, ser. International Series in Operations Research & Management Science. New York, NY: Springer, 2013.
- [15] M. Bagajewicz and V. Manousiouthakis, "On the generalized Benders decomposition," *Comput. Chem. Eng.*, vol. 15, no. 10, pp. 691–700, Oct. 1991.
- [16] J. R. Birge and F. V. Louveaux, "A multicut algorithm for two-stage stochastic linear programs," *Eur. J. Oper. Res.*, vol. 34, no. 3, pp. 384–392, Mar. 1988.
- [17] J. Fortuny-Amat and B. McCarl, "A representation and economic interpretation of a two-level programming problem," *J. Oper. Res. Soc.*, vol. 32, no. 9, pp. 783–792, Sep. 1981.
- [18] T. V. Jensen, J. Kazempour, and P. Pinson, "Cost-optimal ATC code," 2016. [Online]. Available: <https://github.com/TueVJ/Bilevel-ATC>
- [19] C. Grigg, P. Wong *et al.*, "The IEEE reliability test system-1996. A report prepared by the reliability test system task force of the application of probability methods subcommittee," *IEEE Trans. Power Syst.*, vol. 14, no. 3, pp. 1010–1020, 1999.
- [20] T. V. Jensen, P. Pinson, M. Greiner, and H. de Sevin, "The RE-Europe data set," 2015. [Online]. Available: <https://zenodo.org/record/35177>
- [21] ACER, "ACER opinion 09-2015 on the compliance of NRAs' decisions approving methods of cross-border capacity allocation in the CEE region," Tech. Rep., 2015.
- [22] Nord Pool, "Nord pool spot: Market data," 2016. [Online]. Available: [www.nordpoolspot.com](http://www.nordpoolspot.com)